

INVESTIGATION OF THE COMPLEX THERMAL BEHAVIOR OF FATS

Combined DSC and X-ray diffraction techniques

*G. Keller**, *F. Lavigne**, *C. Loisel**, *M. Ollivon*¹* and *C. Bourgaux***

*Equipe Physico-chimie des Systèmes Polyphasés, URA 1218 du CNRS, 5, rue J-B. Clément, 92296 Chatenay-Malabry

**Laboratoire pour l'Utilisation du Rayonnement Electromagnétique (LURE) Université Paris-Sud, BP 209D, 91405 Orsay Cedex, France

Abstract

The thermal behavior of three ural fats (displaying very different composition), cocoa butter (CB)², lard, and a stearin obtained from anhydrous milk-fat (AMF) fractionation, were studied by both DSC and X-ray diffraction as a function of temperature (XRDT). To perform temperature explorations between -30°C and +80°C, at rates identical to those used for DSC and ranging from 0.1 K min⁻¹ to 10 K min⁻¹, a new set of X-ray sample-holders, temperature-controlled by Peltier effect, has been developed. It is shown that the three more stable polymorphic forms of CB were easily characterized by either X-ray diffraction or DSC, and existence of two β -3L forms was confirmed. On the contrary, the more complex polymorphism of lard and AMF required combined examination by DSC and XRDT and the brightness of the synchrotron source for studies at the highest heating rates. Quantitative analysis of the long spacings of XRDT recordings is invaluable for interpretation of thermal events. For instance, it was found that the simultaneous formation of two polymorphic forms, of apparent long spacing of 34 and 42 Å, at the onset of lard crystallization might explain the difficulty of its fractionation.

Keywords: cocoa butter, fat crystallization, DSC, fat polymorphism, fat structure, fats, lard, milk fat, triacylglycerols, X-ray diffraction

Introduction

Natural fats are composed of mixtures of numerous triacylglycerols (TAG) (or triglycerides), which are triesters of glycerol and fatty acids. They fre-

1 Author to whom all correspondence should be addressed.

2 Abbreviations: AMF=anhydrous milk fat; CB=cocoa butter; DSC=differential scanning calorimetry; LS=long spacing; SS=short spacing; TAG=triacylglycerol; XRD=X-ray diffraction; XRDT=X-ray diffraction as a function of temperature.

quently exhibit complex temperature-dependent properties in relation to fat composition and specific TAG behaviors. Cocoa butter is one of the simplest TAG mixtures with respect to composition, with only three monounsaturated triacylglycerols accounting for about 80% of its molar composition. On the other hand, more than 200 different TAGs have been identified in milk fat [1]. However, all fats, even those composed of only a few TAGs, such as cocoa butter, exhibit very complex thermal properties [2]. Indeed, this complexity, which is related to fat composition, is, however, drastically enhanced by the existence of polymorphism of a monotropic type for each TAG [3, 4].

When calorimetry is used for the investigation of thermal properties of fats, several peaks are often observed on heating or cooling of samples. These peaks reflect the occurrence of numerous thermal transitions [5]. These complex recordings, which are not easily interpretable, depend on heating or cooling rates and on the entire thermal history of the sample [6]. Moreover, as a function of conditioning, several polymorphic crystalline species are observed for each pure TAG, and mixtures of TAGs may form mixed crystals, the structures of which are different from those formed by the pure compounds. In that case, identification of the species, the domain of existence of which is delimited by each DSC melting or crystallization peak, is rather complicated and often quite impossible without the aid of techniques that yield information about structures (e.g. X-ray or neutron diffraction, Infrared spectroscopy, etc.) [7, 8]. In this respect, X-ray diffraction (XRD), which is probably the most convenient technique for structural investigation of TAG polymorphism, provides two types of information that help in the interpretation of the thermal events [9, 10].

At low angles, a series of diffraction lines, the intensities of which depend on the Miller indices of the diffracting planes and their structure factors, is observed for each type of crystal [9, 11]. These diffraction lines correspond, for lipids, to the so-called long spacings (LS), and they are indicative of the longitudinal packing of molecules. Lipid molecules stack in parallel, one next to the other, to form layers, the thickness of which depends on the length of the chains, their similarity (in fact, their ability to pack together), and the presence of "potential defects for packing", such as unsaturations or ramifications, along the chains. Thus, the thickness of these layers is primarily related to the number of chains stacked one on top of the other. For TAGs, this number frequently takes a value of 2, 3 or 6 [3, 12].

At larger angles, the observed lines (the so-called short spacings (SS)) reflect the lateral organization of the chains. Since chains can pack laterally in more than 6 different ways, depending on their unsaturation and the sample's thermal history, these lines frequently overlap, especially at low temperatures, at which all TAGs are crystalline, which makes very difficult the interpretation of X-ray patterns [3, 12].

To solve the difficult problem of correctly interpreting both the diffraction patterns and the thermal analysis recordings, it is necessary to compare structural information obtained at different temperatures [13, 14]. This comparison allows one to tentatively attribute the absence or presence of a set of diffraction lines, and the peaks of their corresponding melting transitions, to defined crystalline species. In this respect, recording of XRD films as a function of temperature, using specific cameras, recently permitted visualization and interpretation, at least on a qualitative basis, of the different phase changes involved during fat-melting processes. Concerning these recordings, it should be noted that certain interpretations become very difficult, when species instability, caused by rapid crystallization or improper tempering conditions, exists in the mixtures. In such a case, wherein monotropism of TAGs results in equilibrium not being reached in the whole sample, unstable species transform into more stable ones during the course of the recording, resulting in a complicated overlapping of crystallization and melting peaks, which makes interpretation difficult [13, 15].

In this paper, we first describe two sample holders developed for quantitative XRD-recording as a function of temperature (XRDT), during either fast or slow, heating or cooling, scans. Then, some selected examples are given of the use of such recordings, for interpretation of the complicated behavior of fat, in parallel with DSC measurements obtained under the same conditions. The overall results demonstrate the complementarity of these techniques and the necessity of such coupling and quantitative analysis for the study of thermal properties of natural fats.

Materials and methods

Samples

Pure cocoa butter (Ivory Coast), lard (from CTSCCV, Maisons-Alfort), and primary stearin, resulting from anhydrous milk fat (AMF) fractionation of winter butter (from ADRIA Normandie), were analyzed as received. Form IV of cocoa butter was obtained, after 2 h storage at 50°C, by cooling to 18°C for 2 h, followed by overnight storage at 5°C. Form V was prepared by cooling liquid cocoa butter from 45°C to 28°C and then heating it to 31°C. Form VI of cocoa butter corresponds to a sample stored for several years at room temperature. When not otherwise specified, the thermal history of all samples was systematically destroyed by tempering for 10 min at 10°C above their melting point.

Thermal analysis

A complete study of the complex polymorphism of natural fats require one to examine samples, the stability of which ranges, from fully unstable to species

at equilibrium. Therefore, there is a need to employ different heating and cooling rates; the more unstable the species, the faster the rate. Three types of apparatus were used for thermal analysis, depending on the desired scan rates. A DSC 4 (PERKIN-ELMER), equipped with a cryoson N₂ cooler, and a METTLER (TC 10A) thermal analyser were used for fast recordings (with AMF and CB, respectively), while a calorimeter of the heat-flux type (ARION) was used for 0.1 K min⁻¹ scans (lard). Samples were contained in aluminum pans or other specific sample-holders (about 5–10 or 100–200 mg, respectively). All three calorimeters were calibrated for temperature and enthalpy using ultrapure lauric acid, as described previously [16]. Thermal analysis of cocoa butter was conducted, between -20°C and 50°C at 5 K min⁻¹, with the Mettler analyser (the only one available on site at the time of measurement). For each analysis, a single piece of cocoa butter (20±1 mg) was contained in an aluminum pan (40 µl), in order to optimize repeatability, since the recording of double endotherms could be due to different thermal contacts of multiple sample pieces with the pan. The loading of the unstable cocoa butter sample (form IV) was made at 4°C by direct transfer from a cold chamber to the DSC sample-holder, in order to avoid any polymorphic transition to a more stable species such as form V. Under these conditions, repeatability of DSC scans on replicate samples was better than 0.3°C for temperature and 3% for enthalpy measurements.

X-ray diffraction

Cocoa butter samples were placed in a sample-holder (the temperature of which was water-controlled) developed for reflection analysis. In order to increase resolution at larger angles, 10 to 20 runs were accumulated overnight under conditions defined below. Diffraction patterns were obtained between 0.42° and 15.42° (θ). Analysis of forms IV and V was done at room temperature (20°C), and that of form IV at 16°C. Other samples, which were analyzed by transmission, were loaded in thin glass capillaries (GLAS, Muller, Berlin, Germany) (0.01 mm wall thickness, diameter < 1.5 mm), by means of centrifugation (500 to 1000 rpm) after sample melting. In those cases in which the sample was sensitive to oxidation (e.g. lard), it was kept under argon and the capillary was sealed with a drop of melted paraffin.

In our lab, two sample-holders have been specially developed for XRD as a function of temperature. Both utilize the Peltier effect³ for cooling, with con-

3 As opposed to temperature measurement using a thermocouple created by the junction of two different metals, which transforms a temperature difference into DC voltage, the Peltier effect transforms DC voltage applied to a thermocouple into heating or cooling, depending on the direction of the current. Flat Peltier devices, such as those used here, are made from a series of high-yield thermocouples. These devices, when powered by a few electric watts (typ. 6 V, 2.5 A), are able to generate temperature difference of more than 50°C between the two faces of the battery. In contrast to the Joule effect, which is only used for temperature control by heating, the Peltier effect provides both heating and cooling.

stant voltage applied to the thermoelectric heat-pump modules (Melcor, NJ), and the Joule effect for heating and regulation. The sample-holder shown in Fig. 1a was used for slow heating and cooling rates; it was placed in the center of a goniometer (Seifert, Germany), which was monitored by a computer and equipped with scintillation detection (EG&G). Intensities were recorded at 0.01° intervals, using specific PC software [17]. The K_{α} Cu radiation ($\lambda=1.5405 \text{ \AA}$), obtained under 40 kV and 20 mA conditions was Ni-filtered but not monochromated, for both XRD and XRDT recordings using a conventional X-ray source. The D24 bench of the DCI synchrotron of LURE was used for fast XRDT studies ($\lambda=1.489 \text{ \AA}$) [14, 15].

In these sample-holders, circulation of a water+ethanol mixture (W in Fig. 1) is used to maintain at low temperature the thermoelectric heat-pump modules (P) that cool the sample-holder (S). This allows one to cool the samples to about -30°C with single-stage thermoelectric devices, using a $+5^\circ\text{C}$ circulating mixture. Temperature control of the sample (to within 0.1°C) and scan rates ranging from 0.1 to 5 K min^{-1} are obtained by connecting the heating coil (H) and thermocouple (T) to a computer-driven thermal controller

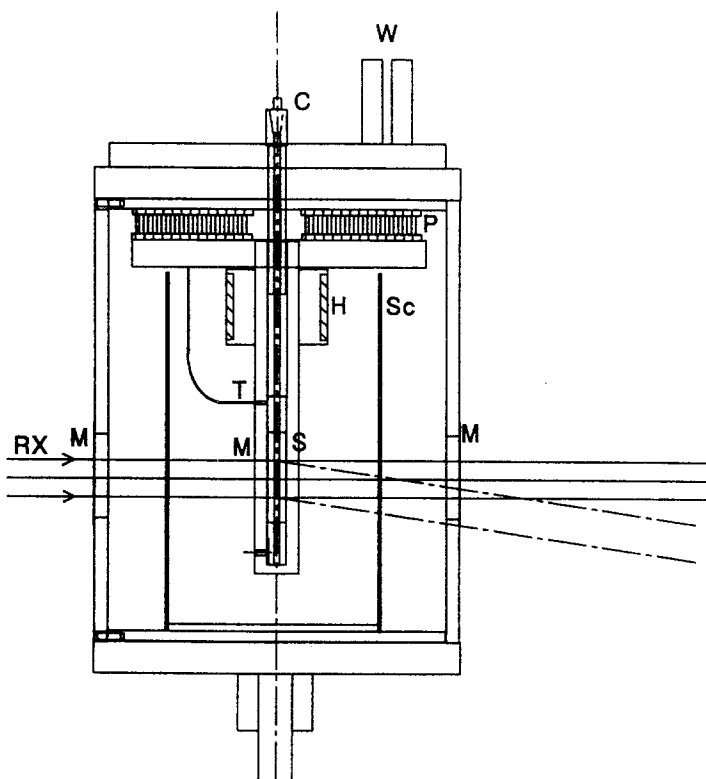


Fig. 1 Experimental set-up of the temperature-controlled sample-holders used for X-ray diffraction studies: a) with conventional X-ray tube at low scanning rates

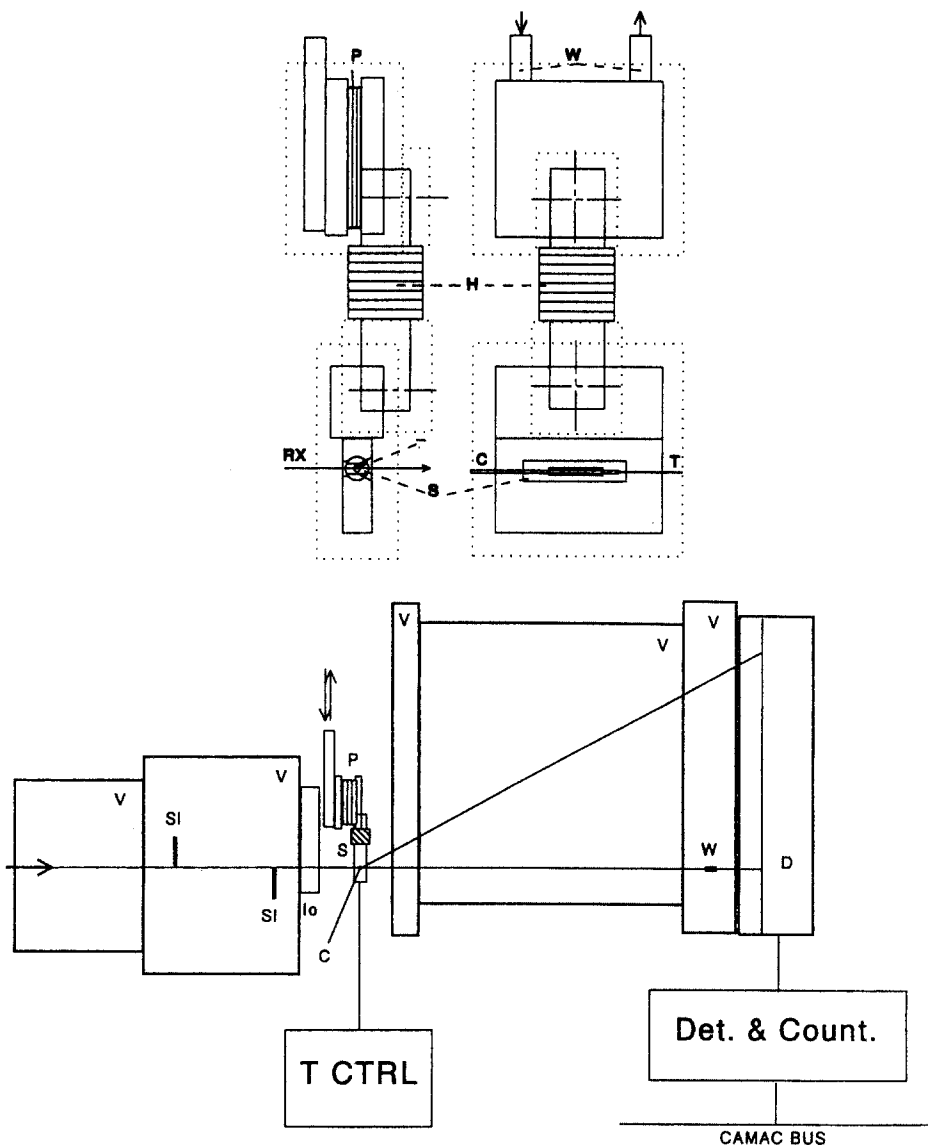


Fig. 1 Continued: Experimental set-up of the temperature-controlled sample-holders used for X-ray diffraction studies: b) with X-ray synchrotron at high scanning rates; c) set-up of the D24 bench used at LURE for the study of TAG polymorphism (C is the capillary of the sample-holder, S, of Fig. 1b, W is the beam stop made of a tungsten bar 3 mm wide and 1mm thick, S1 are slits)

(EUROTHERM, 902P). In both sample-holders, mylar films (four screens of 15 μm thickness each, two on each side) (M) are used for thermal insulation in the direction of the X-ray beam. The thermal screen (Sc), which is used at high

temperature, was removed for these low-temperature experiments. Sample capillaries (C) are centered and adjusted in the beam by moving a capillary holder up or down (Fig. 1a).

The temperature-controlled sample-holder used for fast experiments with the X-ray synchrotron was more compact, as shown in Fig. 1b, because it had to be inserted in as narrow as possible space between tubes kept under vacuum (v) (Fig. 1c). This holder was polystyrene-insulated; the beam also passed through four mylar screens (15 μm). A 1024-channel linear detector (De), using an Ar + CO₂ mixture as the gas stream, was used for detection. Data were collected through a Camac bus linked to a microvax computer. This equipment allows one to obtain, from the same experiment, up to 24 frames of the same duration (from 1 to 2000 s), each separated by 1 sec of data logging. Temperature, measured by the thermocouple and transmitted by the thermal controller, was recorded as a function of thermal treatment, using a laptop computer.

Results and discussion

The complete study of complex monotropic polymorphism of natural fats require one to examine all species that might be formed under any conditions. This leads to characterizing samples, the stability of which ranges from unstable to samples at equilibrium. Inevitably, since this stability is time- and temperature-dependent, the study of unstable species results, under certain conditions, in their transformation to more stable ones. Therefore, to avoid, limit to some extent, or cause these transformations, as well as on the contrary to keep melting species close to equilibrium, there is a need to examine samples at different heating and cooling rates: as a rule of thumb, the more unstable the species, the faster the rate should be. How can one characterize such species under these conditions? In practice, it is well known by thermal analysts that no universal equipment allows one to perform studies at both high and low scanning rates. Therefore, two types of apparatus were used for thermal analysis, the choice depending on the desired scan rates; also, two specific pieces of equipment were specially developed in this laboratory for XRDT studies (described earlier).

To illustrate the need for such an approach to the study of fat polymorphism, three natural fats, representing increasing complexity in triacylglycerol composition, were examined. For the sake of brevity, only selected aspects of the polymorphism of these natural fats were studied. Cocoa butter (CB) has the simplest composition; about 75% of the TAGs are monounsaturated and correspond to three major compounds, POP, POS, and SOS⁴ [18]. AMF certainly has the most complex composition; more than 400 different fatty acids have

⁴ TAGs are commonly designated by three letters which correspond to the fatty acids esterifying the 1, 2, and 3 positions of glycerol: M is for myristic, P for palmitic, S for stearic, O for oleic, L for linoleic; for instance, PSS is 1-palmitoyl, 2-3, distearoylglycerol.

been identified in butter fat. Each of these fatty acids has the possibility, at least in theory, of being esterified in each of the three positions of glycerol; thus, thousands of TAGs could possibly be identified in butter. However, among the 200 already identified, only several (probably, 5 to 9) are present in amounts larger than 2% [1, 19–23]. Lard fat is of intermediate complexity; three TAGs (POL, POO, and PSO⁴) account for 60% of the total composition. However, contrary to what is observed for CB, all three belong to different classes of TAGs, from monounsaturated to triunsaturated [18]. All three fats are solid-like at room temperature, and their melting is completed at temperatures in the range from 35 to 50°C.

Cocoa butter

The specific thermal behavior of CB, with four [24] to six [25, 26] crystalline forms characterized (denoted by Lutton as I to VI, in the order of increasing melting points), originates from that of its main monounsaturated TAG. In this respect, POP⁴ exhibits at least six different crystalline polymorphic species [27]. Indeed, only the more stable ones (IV to VI) are of importance for processing of chocolate-containing food products. Since cocoa butter crystallization cannot be achieved directly to the two more stable β forms, V and/or VI, it is necessary to reach this state progressively by step-by-step conditioning, in a process called tempering. During this process, CB is slowly crystallized in a mixture of IV and V forms, which slowly, during subsequent cooling and storage, completely transforms into V, before eventually reaching the VI form, which is not necessarily desired [28, 29]. The initial step consists of developing enough seed crystals in the chocolate mass to allow fast and homogeneous crystallization during the cooling stage.

The three endotherms shown in Fig. 2a correspond to the melting curves measured at 5 K min⁻¹ for forms IV, V and VI of cocoa butter. Melting temperatures of these three species range from about 25 to 33°C. Form IV of cocoa butter is characterized by a melting temperature ranging between 25 and 27.5°C, [25, 30]. Melting temperatures of forms V and VI are located between 30 and 36°C, and are less than two degrees apart for these two crystalline forms. For this reason, some authors combine forms V and VI of cocoa butter into a single polymorphic form characterized by a melting temperature ranging between 33.7 and 34.9°C [24].

The presence of single, sharp, endothermic peaks is characteristic of the melting of crystals formed from only a few TAGs of high compatibility. This is the case for fats such as cocoa or coconut butter, which are composed of relatively few triacylglycerols of similar chain length, in comparison to other fats, such as the two examined below. The three sharp endotherms observed correspond to the melting of different polymorphic forms produced essentially by the

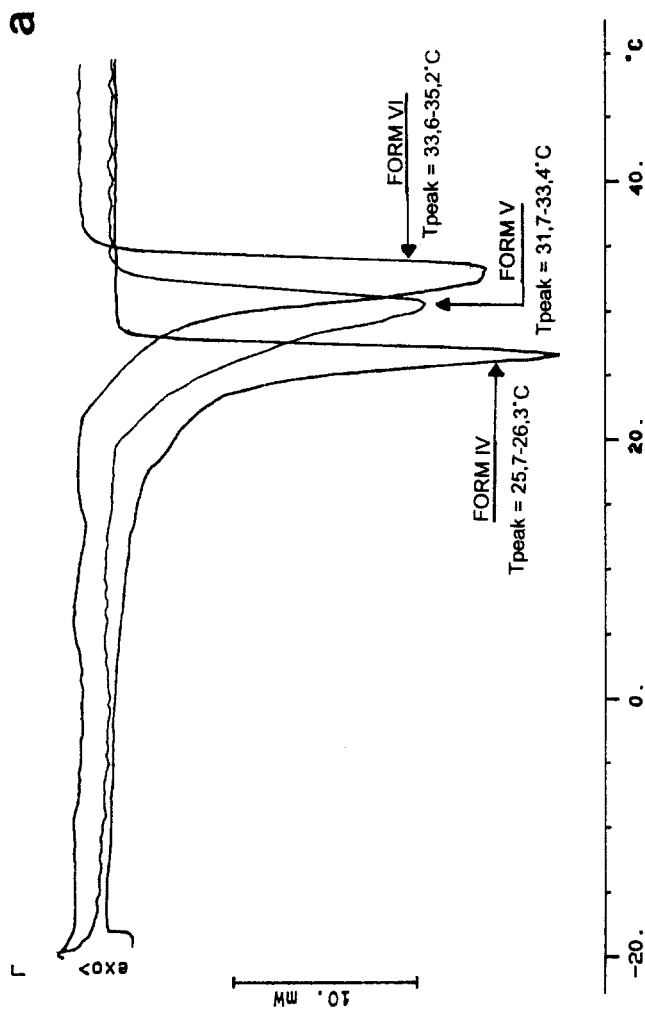


Fig. 2 TAG polymorphism, as illustrated by the three more stable species of cocoa butter:
 a) Mettler DSC recordings, obtained at 5 K min⁻¹, for forms IV to VI of cocoa butter. If we disregard baseline drift, likely related to the progressive solubilization of the monounsaturated TAGs into the liquid-remaining fraction of the fat, we see that each form exhibits a single melting peak

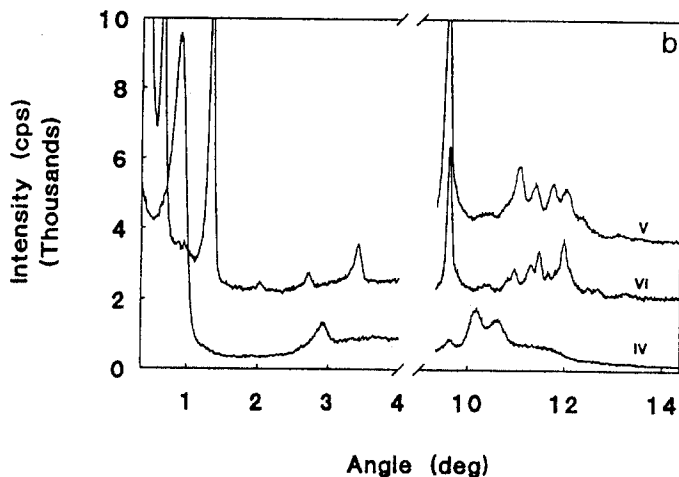


Fig. 2 Continued: TAG polymorphism, as illustrated by the three more stable species of cocoa butter: b) corresponding XRD recordings. For clarity, the LS pattern of form V, which is almost identical to that of form VI, is not shown. The LS of species IV and VI illustrate the difference in packing between 2L and 3L, respectively

three main triacylglycerols: POP, POS, and SOS⁴. As mentioned above, identification of the three more stable species of cocoa butter from their melting temperatures is a problem that could be addressed by DSC, provided that the forms are first determined properly by XRD.

Figure 2b shows X-ray diffraction patterns of forms IV, V and VI of cocoa butter. Form IV, which corresponds to a β' structure with two alkyl chains per layer (2L), is characterized by broad diffraction peaks, LS=45 Å ($\theta \cong 1^\circ$) and SS=4.35 Å ($\theta \cong 10.2^\circ$) and 4.15 Å ($\theta \cong 10.6^\circ$) [25–29]. Forms V and VI, which both correspond to a β structure with three alkyl chains per layer (3L), show LS \cong 65 Å ($\theta \cong 0.7^\circ$). According to different authors, these two forms show a similar LS value [25] or two distinct values in the range 63–66 Å [28, 29]. According to a recent study [31], forms V and VI correspond to different conformations of oleic acid in unsaturated triacylglycerols such as SOS⁴. In addition to the "normal" bent structure of oleic acid, a straighter conformation, which differs in the conformation around carbon 11, was defined. Those authors also suggested that the phase transformation of V to VI in cocoa butter was responsible for the formation of "bloom" on chocolate, and that it involved a change in the layer stacking, resulting in a higher crystal symmetry.

Lard

Lard is a fat that displays a final melting temperature above 40°C. At room temperature, shortenings made from natural lard characteristically have a waxy or grainy texture and exhibit unsatisfactory cake-baking qualities. Direct frac-

tionation of lard, which might improve the characteristics of its fractions, is known to be quite difficult without the help of solvent or chemical pretreatment of the fat, such as by interesterification [32]. Lard's composition is characterized by high contents of trisaturated TAGs with long chains (e.g. 2–10% of SPS+PSS⁴), the melting temperatures of which, as pure compounds, exceed 60°C [3, 18]. These saturated compounds are more or less solubilized, depending on the thermal history of the fat, at temperatures above 40°C by the large amounts of liquid disaturated (36%) and monosaturated (43.5%) TAGs.

Whatever the scanning rate, lard crystallization occurs in several steps. Rapid cooling, at 5 K min⁻¹, leads to two exothermic peaks (data not shown) of similar enthalpies, corresponding to a two-step crystallization. The first peak, which is preceded by a small double shoulder at 14 and 12°C, occurs at 11°C,

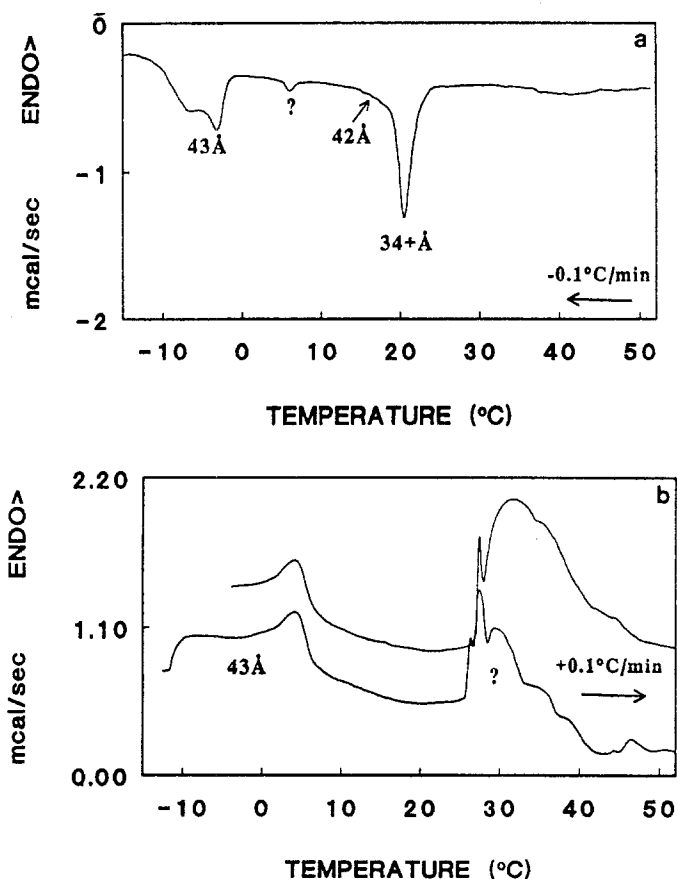


Fig. 3 DSC and XRDT recordings obtained at 0.1 K min⁻¹ for lard exhibit multiple thermal events: a) DSC recording of crystallization: LS indicated near each exotherm have been obtained from the analysis of XRDT data (Fig. 4); b) DSC recording of the corresponding melting

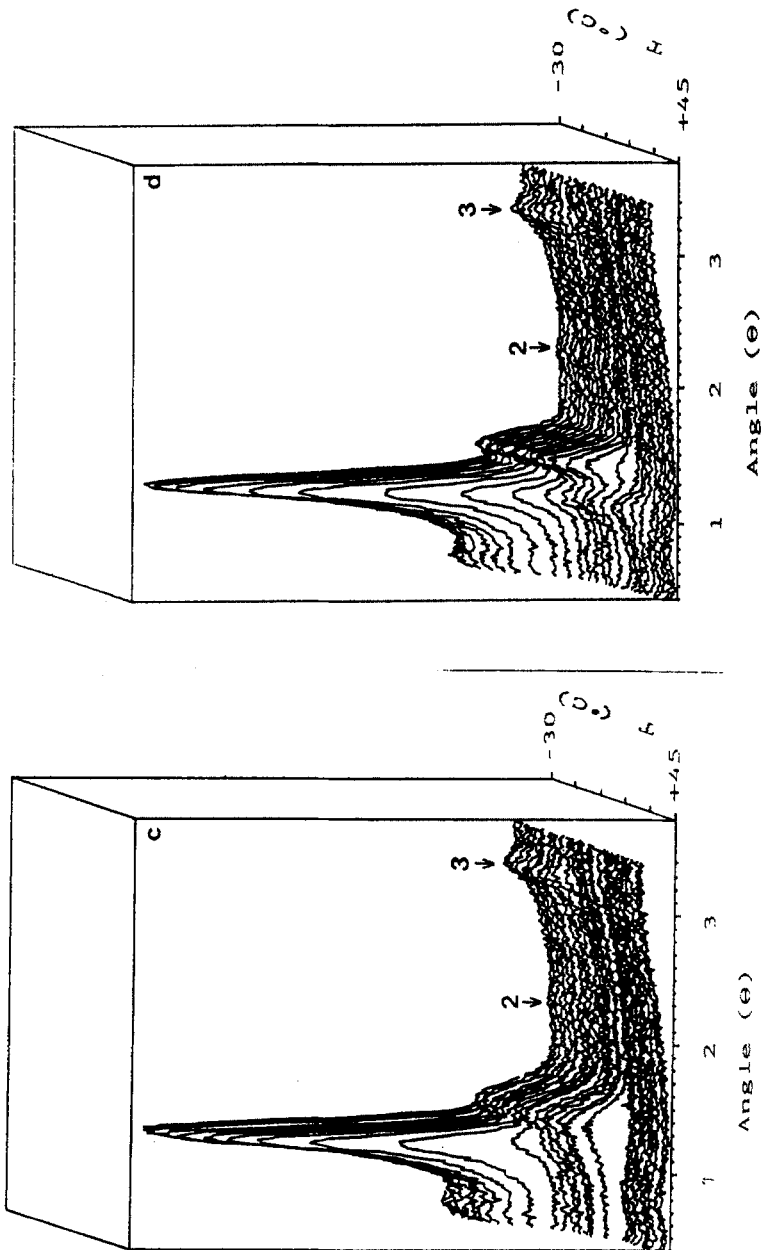


Fig. 3 Continued: DSC and XRD recordings obtained at 0.1 K min^{-1} for lard exhibit multiple thermal events: c) three-dimensional plot of X-ray diffraction recordings taken as a function of time every $30'$ during the cooling at 0.1 K min^{-1} of a sample contained in a capillary tube; d) same as (c), but recorded during the corresponding heating; arrows indicate second (2) and third (3) order lines of the main LS

and the second occurs at -15°C . Melting at 5 K min^{-1} is characterized by two endotherms starting at -4 and 25°C . Both of these peaks are preceded and/or followed by small endothermic bumps (-15 , 18 and 35°C). Contrary to what is observed for CB, lard TAGs seem to separate into different crystalline species, the crystallization and melting temperatures of which cover about a 60°C range.

Such rapid cooling rates are known to lead to the formation of unstable α forms. On heating, such crystalline species are known to transform, due to monotropism and the presence of a liquid phase that accelerates the transition, into more stable β' and/or β forms. Subsequent DSC recordings exhibit both normal melting and polymorphic transitions. Since it is quite difficult to ensure that no polymorphic transition was taking place during melting, interpretations of simple DSC recordings are rendered questionable. XRD analysis of the sample is then required to determine structure changes during DSC measurements. Indeed, identification is possible when single species, evidenced by DSC, are confirmed with static XRD, as was done for CB above. When complex recordings with multiple species are observed, XRDT seems to be a better tool for investigation. The two examples described below were recorded using this technique on two different apparatus and at different scanning rates. Lard (Figs 3 and 4) was studied at low scanning rates, while AMF (Figs 5 and 6) was studied at high ones.

Analysis of lard polymorphism was performed by XRDT, using conventional X-ray apparatus. As the latter does not allow fast recording, due to the low power of the X-ray source, patterns were taken every 30 min, for either 3° or 15° (θ angle) excursions of the goniometer detector. In the former case, which

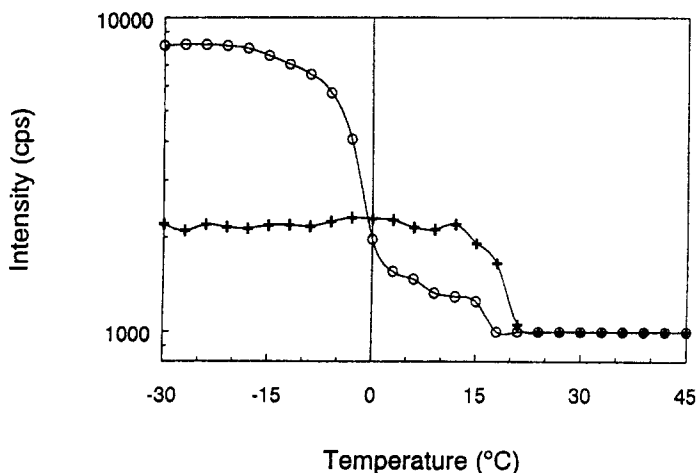


Fig. 4 Quantitative analysis of the X-ray diffraction of lard, recorded as a function of temperature during cooling at 0.1 K min^{-1} (XRDT of Fig. 3c) $+ = 34\text{ \AA}$, $o = 42\text{--}43\text{ \AA}$ (null diffraction, observed at temperatures beyond melting points of the two species, is arbitrarily normalized to 1000 cps for clarity of log plots⁵)

yielded better signal-to-noise ratio, analysis was done during two different experiments, one for low angles and one for high, using 0.1 K min^{-1} scanning rates. Figure 3c shows a three-dimensional recording of lard crystallization at 0.1 K min^{-1} , as followed by XRD vs. temperature. The corresponding DSC analysis recorded at the same cooling rate is shown in Fig. 3a. Both analyses demonstrated multiple crystallization events. While five endotherms were visible on DSC recordings, up to five diffraction lines were observed by XRDT, some of them representing different orders of the same series of diffracting planes (i.e. 00l). These XRDT data were analyzed quantitatively, by plotting intensities of the two main lines, observed near 1° angle, as a function of temperature (Fig. 4). Such a plot allows one to determine the onset and completion temperatures of crystallization (or melting) of each polymorphic form, and then, by comparison to the corresponding thermal events, to identify these thermal events unambiguously.

The occurrence of the different polymorphic forms as a function of cooling is clearly depicted on these diagrams and can be summarized as follows. An initial, very abrupt crystallization starts at $21\text{--}22^\circ\text{C}$ and is immediately followed by a more gradual one developing around 19°C . These two crystallizations, the peaks of which are overlapping on the DSC recording, are clearly separated by XRDT and correspond to 34 and 42 Å LS, respectively. Around 0°C , new crystals develop in two steps (clearly shown in Figs 3a and 3c), the first one again being sharper than the second. The latter peaks apparently correspond to similar LS (43 Å). In fact, because of the poor angular resolution of XRDT during fast scanning, three different lines (these last two and the previous one at 42 Å) have been plotted together in Fig 4.⁵ Diffraction lines corresponding to a second order of the 42 Å LS and a third order of the 34 Å LS, the presence and relative intensities of which may provide some information about molecular organization within layers [11], are also observed. In this respect, the 34 Å LS might have been, as frequently observed for unsaturated TAGs with long chains (cF. in Fig. 5, a line at 70 Å), the second order of a 68 Å LS corresponding to a three-layered structure. Figure 3c shows that this was not the case, since first-order reflections are absent. Therefore, such packing occurring at relatively high temperature should likely be attributed to long-chain saturated TAGs with a high angle of inclination of the chain relative to the layers. Nevertheless, because of the broadness of the peak at lower angles, a packing not corresponding

⁵ For clarity of drawing, instead of percentage of the total intensity of the diffraction peak (examples of such plots are shown Fig. 6) we preferred to keep the original intensities on a log scale. Such a plot allows better presentation of the different jumps that evidence the successive occurrence of different species of similar LS.

to a unique thickness and regular organization of the molecules, but rather to a distribution of LS, should not be ruled out.

The corresponding DSC melting, recorded at 0.1 K min^{-1} , is shown in Fig. 3b. As expected, the different crystalline species observed on cooling melt in the reverse order of their crystallization, except for the two high-melting peaks (Fig. 3d). Since final melting of the form displaying a 42 \AA LS occurs at a temperature well above its crystallization temperature, a polymorphic transformation during the cooling/heating cycle cannot be excluded. Also, the group of peaks, the melting of which is recorded at temperatures above 25°C , appears very sensitive to the crystallization process and possibly to nucleation phenomena, since these peaks are more numerous than are the polymorphic forms identified. Therefore, unambiguous identification of the polymorphic species was not possible. Further investigations are required to determine more pre-

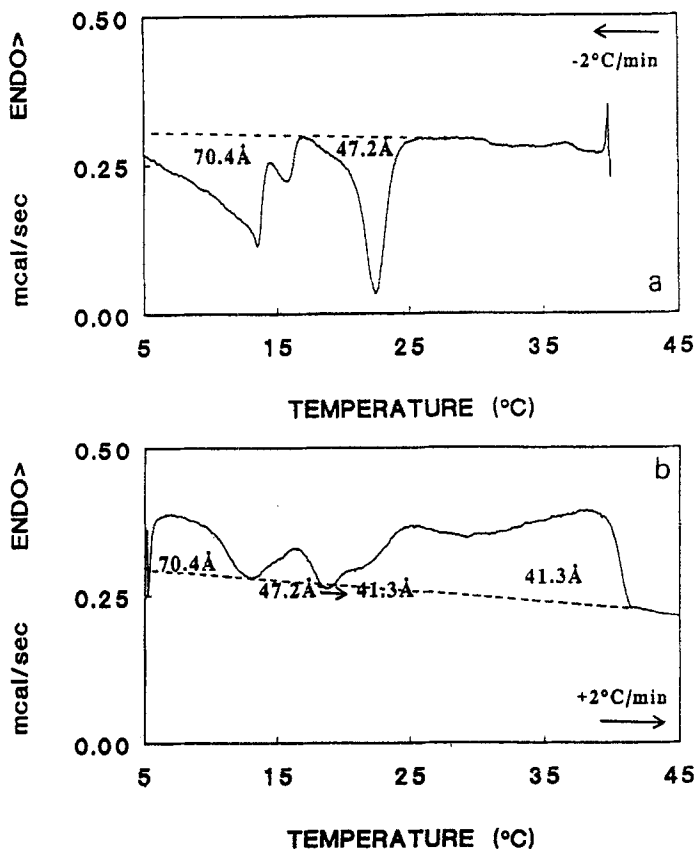


Fig. 5 Thermal behavior of a stearic fraction separated from a winter AMF, as recorded during crystallization and melting at 2 K min^{-1} , using DSC and synchrotron X-ray diffraction: a) and b) DSC analysis on cooling and heating (LS as in Fig. 3a), respectively; c) and d) the same for XRDT analysis

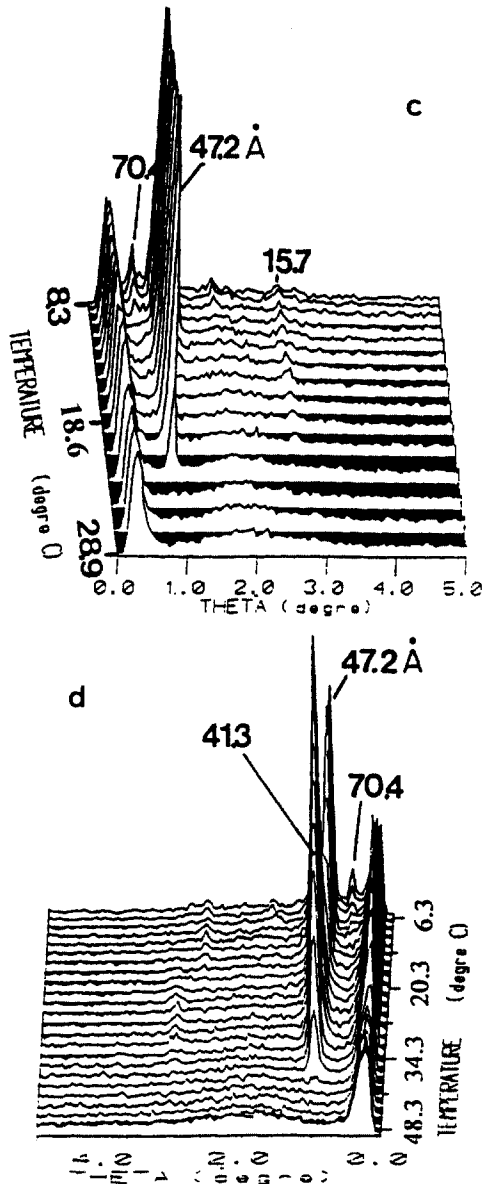


Fig. 5 Continued: Thermal behavior of a stearic fraction separated from a winter AMF, as recorded during crystallization and melting at 2 K min^{-1} , using DSC and synchrotron X-ray diffraction: c) and d) the same for XRDT analysis

cisely the different structural characteristics of the phases. In addition, XRDT, as recorded, has not allowed observation of any diffraction line associated with the crystallization peak observed by DSC at about 6°C . Thus, while XRDT is a

powerful technique that serves to complement DSC measurements by identifying the crystalline forms involved, DSC remains an irreplaceable source of information on thermal events. On the contrary, the crystallization around 20°C, of the two different species evidenced by XRDT could not be detected by DSC. The quasi-simultaneous crystallization of these two forms might explain why lard fat cannot be easily (fractionated, due to the small size of crystals obtained on cooling; fractionation by filtration of liquid fat from solid fat requires large crystals for easy separation). It is possible that the growth of each type of crystal inhibits the growth of the other. This phenomenon might be associated with the separation of solid solutions, observed, for instance, in phase diagrams just below an invariant eutectic temperature.

It is worth noting the excellent correlation between the data obtained by the two techniques, as well as the richness of the information obtained at low angles by XRDT. Lard fractionation and subsequent chromatographic analysis are also needed to determine the TAG compositions of the structures, the crystallization and melting of which are responsible for the different thermal events recorded by both DSC and XRDT. Such analysis, leading to the determination of the major TAGs involved in the structural transformations corresponding to each thermal event, has recently been undertaken for butters of different origins [33]. The following data are part of that study.

Milk fat

AMF is the most complex natural fat, with respect to its TAG composition; as mentioned above, more than 200 individual molecular species of even-numbered TAGs have been recently quantified [1, 19–23]. Since each TAG is characterized by its own melting point, AMF has a broad melting range (approximately -30 to +35°C) and no true melting point. Fractionation of AMF is performed by slowly cooling liquid AMF to a temperature at which the mixture, part liquid and part solid and exhibiting the desired solid/liquid ratio, is separated into two fractions. The low-melting liquid fraction is termed "olein", while the high-melting crystalline fraction is called "stearin". This change in the melting pattern of AMF, brought about by fractionation, is related to the modification of the TAG composition; it has been shown that long-chain monounsaturated and trisaturated TAGs are concentrated in the stearic fraction, while polyunsaturated and short-chain TAGs are found at higher concentrations in the oleic fraction [34–36].

Figure 5a shows the crystallization pattern recorded at -2 K min^{-1} for a stearic fraction separated from a winter AMF. Two main peaks are observed, from 25 to 16°C and from 16 to 5°C respectively. The first one is quite sharp, although a tail is evidenced, while the second one is very broad and starts with a small and partially overlapped exotherm. This signifies that the very complex mixture of TAGs in the stearic fraction of AMF separated itself, during rapid

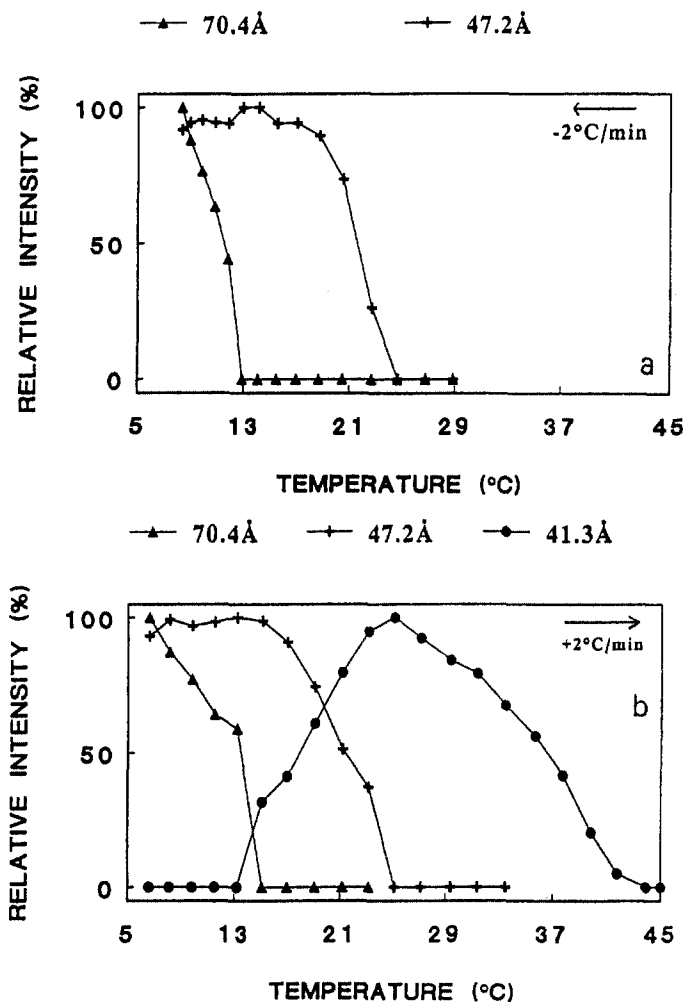


Fig. 6 Quantitative analysis of XRDT data: a) data from Fig. 5c; b) data from Fig. 5d (all diffraction peaks are normalized to 100%)

crystallization, into at least two families. At around 25°C , the corresponding XRDT recording (Fig. 5c) of the LS showed the formation of a crystalline species whose thickness was 47.2 \AA . Once the temperature reached 12°C , one could see the emergence of a second crystalline structure whose thickness was 70.4 \AA . In parallel, the dynamic recording of the SS (not shown) showed the growth of a unique peak at 4.16 \AA indicating that such rapid cooling at -2 K min^{-1} led to the formation of an unstable α form.

The correlation of thermal and structural recordings is possible, as shown in Fig. 6a. Indeed, the relative intensities of the successive $n=1$ peaks observed

during the crystallization of the sample can be plotted on the same scale as that of the corresponding DSC recording as a function of temperature. One can easily see that the first sharp exotherm was related to the formation of a bilayered structure ($2L=47.2 \text{ \AA}$), while the second broad exotherm corresponded to the growth of a trilayered form ($3L=70.4 \text{ \AA}$). According to the literature [3, 4, 12], 2L structures are generated mostly by long-chain, high-melting, trisaturated TAGs, while 3L forms are usually related to low-melting, long-chain, monounsaturated and mixed long- and short-chain TAGs.

Heating this 2L + 3L mixture at $+2 \text{ K min}^{-1}$ led to the complex DSC recording shown in Fig. 5b, in which three broad endotherms are partially overlapped. Peak identification would be impossible without the help of the corresponding XRDT recording (Fig. 5d) and the derived plot of the change in intensity of the first-order peaks as a function of temperature (Fig. 6b). Comparison of Figs 5b and 5d indicates that the low-melting, 3L structure disappeared at the temperatures corresponding to the first endotherm. The 2L form melted beyond 15°C but preceded the formation of a new set of diffraction lines indicative of a recrystallization into a thinner bilayer (41.3 \AA). This polymorphic transition, $47.2 \rightarrow 41.3 \text{ \AA}$, could be located on the thermogram, because it was related to a wholly exothermic signal going transiently under the baseline (Fig. 5b). The new 2L structure was more stable than the previous one and was therefore responsible for the high-temperature melting peaks, the final temperature of which reached 43°C .

Application of combined XRDT-DSC to an AMF fraction has shown that, even in the case of complex fats, complementary structural identification allows one to better understand intricate DSC recordings. Indeed, it is possible to describe the recordings obtained at any typical scan rate in terms of structural parameters, and to decipher complex, overlapping endo and exothermic events. Furthermore, the structural parameters provided by the XRDT recordings can be related to the TAG composition of the successive crystalline forms whose crystallization and melting are recorded, since their thickness is a function of the mean chain length, the angle of inclination, and the packing of the different families of TAGs composing AMF. We will soon publish a series of papers in which this relationship between thermal and structural parameters and the TAG compositions of products derived from AMF has been studied more fully [36].

The exact determination of onset and completion temperatures by combined techniques remains difficult, because of the use of two different apparatus and samples for DSC and XRDT measurements (uncertainties of temperature determinations by the two techniques should be added when expressing the accuracy of events). In addition to the fact that there is a need to prepare two samples, the thermal histories of which, before and during analysis, are never strictly the same, the space and time separations of these analyses undoubtedly complicate

comparison of their results. Indeed, the present study emphasizes the need for developing a true coupling of the two techniques. Such an apparatus, using the Peltier effect for both temperature control and detection of the thermal analysis signal while XRDT is performed using a synchrotron beam, has just recently been developed. First results obtained for phospholipids, TAGs, and starches will soon be published [37].

Conclusion

The development of new research tools to record both X-ray diffraction as a function of temperature and a broad range of scanning rates in DSC investigations had resulted in excellent agreement between the two techniques. Indeed, coupling of DSC and XRDT is absolutely essential to identify the structures involved in the complex transitions of TAGs, which result from their complex polymorphism, because these transitions frequently overlap, leading to ambiguity in the interpretation of recorded data. In this respect, we have shown that the understanding of thermal recordings is greatly facilitated by the use of XRDT, especially at small angles for LS determinations. Quantitative interpretation of X-ray patterns results in thermal plots, which when compared to DSC thermal plots, allow unambiguous interpretation of the DSC data. However, while the XRDT technique allows a better understanding of the phenomena, it cannot replace the DSC technique, which remains more sensitive to low-energy thermal events.

* * *

Special thanks to Courtney P. Mudd (NIH, Bethesda) for his pertinent advice on the mounting and use of thermoelectric devices. The study of lard crystallization was initiated by Valerie Portalier and suggested by Jean-Luc Vendevre of CTSCCV (Maisons-Alfort). For the AMF part of this study, stearin was fractionated by ADRIA Normandie, while characterization of its thermal properties was performed as part of a research program funded by ARILAIT Recherches and the French Ministry of Research and Technology.

References

- 1 J. Gresti, M. Bugaut, C. Maniongui and J. Bezar, *J. Dairy Sci.*, 76 (1993) 1850.
- 2 V. D'Souza, J. M. De Man and L. De Man, *J. Am. Oil Chem. Soc.*, 67 (1990) 835.
- 3 D. M. Small, *The Physical Chemistry of lipids. From alkanes to phospholipids*, Plenum Press, New York 1986, chap. 10.
- 4 M. Ollivon and R. Perron, *Manuel des corps gras*, AFECG, A. Karleskind and J. P. Wolff, Ed., Lavoisier, Paris 1992, chap. 5.
- 5 A. R. M. Ali and P. S. Dimick, *J. Am. Oil Chem. Soc.*, 71 (1994) 803.
- 6 M. Ollivon and R. Perron, *Fat Science, Part A*, A. J. Hollo ed., Elsevier (1985) p. 107.
- 7 J. M. De Man, *Food Res. Int.*, 25 (1992) 471.
- 8 R. E. Timms, *Aust. J. Dairy Technol.*, 35 (1980) 47.

- 9 A. Guinier, *Théorie et Technique de la Radiocristallographie*, 3ème édition, Dunod, Paris 1964.
- 10 M. van Meersche and J. Feneau-Dupont, *Introduction à la Cristallographie et à la Chimie Structurale*, 3ème édition, Peeters, 1984.
- 11 M. Ollivon, *Thèse de Doctorat d'Etat*, Paris VI (1982).
- 12 J. W. Hagemann, in *Crystallization and Polymorphism of Fats and Fatty Acids*, N. Garti and K. Sato, eds., Marcel Dekker, NY 1988.
- 13 M. Kellens, W. Meeussen, C. Riekel and H. Reynaers, *Chem. Phys. Lipids*, 52 (1990) 79.
- 14 F. Lavigne and M. Ollivon, *Proc. Journées Méditerranéennes Calorimétrie Analyse Thermique*, Corte, Sept., AFCAT, vol. XXIV (1993) 237.
- 15 F. Lavigne, C. Bourgeaux and M. Ollivon, *J. Phys.* IV, 3 (1993) 137.
- 16 C. Grabielle-Madelmont and R. Perron, *J. Colloid Interface Sci.*, 95 (1983) 471.
- 17 B. Ducourant, B. Fraisse and R. Fourcade, X-ray computer programs "Rayon" et "Relief", *Laboratoire Chimie Minérale, Université Montpellier II* (1993).
- 18 A. Karleskind and J. P. Wolff, *Manuel des Corps Gras*, Tome 1, AFECG, Lavoisier, Paris 1992, chap. 3.
- 19 S. Kuzdal-Savoie, *La Technique Laitière*, 992 (1984) 43.
- 20 F. Dorey, D. Brodin, J. F. Le Querler and S. Kuzdal-Savoie, *Ind. Agro-Alim*, 105 (1988) 437.
- 21 P. H. Laakso, K. V. V. Nurmela and D. R. Homer, *J. Agric. Food Chem.*, 40 (1992) 2472.
- 22 S. Bornaz, G. Novak and M. Parmentier, *J. Am. Oil Chem. Soc.*, 69 (1992) 1131.
- 23 S. Bornaz, G. Novak and M. Parmentier, *J. Am. Oil Chem. Soc.*, 70 (1993) 1075.
- 24 G. V. Merken and S. V. Vaeck, *Lebensm. Wiss. U. Technol.*, 13 (1980) 314.
- 25 R. L. Wille and E. S. Lutton, *J. Am. Oil Chem. Soc.*, 43 (1966) 491.
- 26 G. M. Chapman, E. E. Akehurst and W. B. Wright, *J. Am. Oil Chem. Soc.*, 48 (1971) 824.
- 27 K. Sato, T. Arashima, Z. H. Wang, K. Oshima, N. Sagi and H. Mori, *J. Am. Oil Chem. Soc.*, 66 (1989) 1044.
- 28 H. Adenier, M. Ollivon, R. Perron and H. Chaveron, *Chocolaterie Confiserie de France*, 315 (1975) 7.
- 29 J. Schlichter and N. Garti, in *Crystallization and Polymorphism of Fats and Fatty Acids*, N. Garti and K. Sato, eds., Marcel Dekker, NY 1988.
- 30 N. V. Lovegren, M. S. Gray and R. O. Feuge, *J. Am. Oil Chem. Soc.*, 53 (1976) 83.
- 31 S. De Jong, T. C. Van Soest and M. A. Van Schaick, *J. Am. Oil Chem. Soc.*, 68 (1991) 371.
- 32 L. H. Wiedermann, T. J. Weiss, G. A. Jacobson and K. F. Mattil, *J. Am. Oil Chem. Soc.*, 38 (1961) 389.
- 33 F. Lavigne, *Thèse de l'Université Paris-Sud (Orsay)*, 1995.
- 34 D. Brodin, *Thèse de l'Université de Caen* (1989).
- 35 E. Deffense, *J. Am. Oil Chem. Soc.*, 70 (1993) 1193.
- 36 F. Lavigne and M. Ollivon, in preparation (1996).
- 37 M. Ollivon, C. Bourgeaux and G. Keller, in preparation (1996).